

# Optical Properties of TSP: NaNO<sub>3</sub> Biopolymer Electrolyte

Gnana kiran M.<sup>1,2</sup>, Krishna Jyothi N.<sup>1\*</sup>, Samatha K.<sup>2</sup>, Rao M.P.<sup>2</sup> and Vijayakumar K.<sup>3</sup>

1. Department of Physics, Koneru Lakshmaiah Education Foundation, Vaddeswaram andhra Pradesh, INDIA

2. Department of Physics andhra University, Vizag andhra Pradesh, INDIA

3. Department of Physics, Dayananda Sagar University, Bengaluru-560068, Karnataka, INDIA

\*jyothinadella82@gmail.com

## Abstract

Solid biopolymer electrolyte (SPE) film based on biopolymer Tamarind Seed Polysaccharide (TSP) doped with sodium nitrate (NaNO<sub>3</sub>) is developed by solution cast technique. The optical properties have been carried out by UV-visible optical Absorption spectroscopy in the wavelength range of 200-800 nm. From this, the optical absorption, optical transmission, optical absorption coefficient, refractive index spectra, extinction coefficient spectra, direct energy bandgap, indirect energy bandgap, optical absorption edge, estimated bandgap studies are obtained.

The transmittance wavelength is approximately 200nm. The calculated optical band gap changes from 5.01eV to 4.65eV. The optical bandgap indicated that the films are nearly transmitting within the visible range. The direct, indirect and absorption edge for pure TSP is high and by increasing salt concentration of NaNO<sub>3</sub>, the above parameters are observed to decrease gradually. For the concentration of 70% TSP: 30% NaNO<sub>3</sub> low value of direct and indirect energy bandgap is obtained.

**Keywords:** Optical properties, TSP, NaNO<sub>3</sub>, optical absorption, absorption coefficient, direct and indirect band gap.

## Introduction

Basically, material research aims to prepare a new material with properties for an application to understand the chemical, physical and optical behavior that determines these properties<sup>1</sup>. One method to modify the property of a material is doping the biopolymers with a different concentration level of dopant<sup>2</sup>. Biopolymer electrolytes are generally studied for fundamental reasons and practical applications as well. The biopolymer-based electrolytes not only merge the advantageous properties of biopolymers and dopant but also show many new properties<sup>3</sup>. The properties of a biopolymer may be improved and controlled substantially by adding suitable dopants<sup>4</sup>.

Tamarind seed polysaccharide (TSP), which is made from tamarind seeds, is very easily degradable by biological organisms and it is completely soluble in inorganic liquids such as water and ammonia etc<sup>5</sup>. TSP is a natural biopolymer that has been used during the 20<sup>th</sup> century

worldwide<sup>6</sup>. The change in properties due to doping depends upon the chemical nature of the dopant and the kind of interaction between the biopolymer and the dopant<sup>7,8,9</sup>. Tamarind seed polysaccharide is a natural type of polysaccharide obtained from the seeds of Tamarinds Indica, which performs the role of additive, thickener, binder and viscosity enhancer in food and cosmetic industries. TSP contains monomers of glucose, xylose sugars and galactose present in a molar ratio of 3:1:2<sup>10</sup>.

It is soluble in inorganic liquids and is insoluble in organic solvents. It has been used in the commercial, industrial, medical, food sectors and has been used to prepare so many products like packing materials that are regularly in contact with food<sup>11</sup>. TSP is the most biodegradable material imitation of natural biopolymers used in textile sizing and paper coating<sup>12,13</sup>. This biopolymer is widely used by mixing with other polymers and many chemical components for various industrial applications to enhance the optical, electrical and mechanical properties of the membrane because of its compatible structure<sup>14</sup>.

In this work, the optical properties of TSP polymer doped with several concentrations of NaNO<sub>3</sub> are studied. In the present work, optical absorption, optical transition and optical parameters are relatively influenced by processing conditions. There has been no work found using TSP as a host polymer with sodium nitrate conducting the electrolyte<sup>15,16</sup>. In this paper, TSP polymer electrolytes doped with NaNO<sub>3</sub> has been investigated. The structure of the TSP biopolymer is given in fig.1.

## Material and Methods

Tamarind Seed Polysaccharide (TSP) purchased from TCI chemicals, based biopolymer electrolyte films doped with pure sodium nitrate (NaNO<sub>3</sub>) were made in various ratios (90:10) (80:20), (70:30) and (60:40) by solution casting method as double distilled water (H<sub>2</sub>O) as a solvent.

Various concentrations of TSP and NaNO<sub>3</sub> are mixed with double distilled water. The mixture of these solutions was stirred for 12 hours by keeping the temperature at 60°C. Then the homogeneous solution obtained is poured into polypropylene dishes and kept in a vacuum chamber at 60°C. Water in that homogeneous solution was evaporated slowly at that temperature under the vacuum drying process, after 24 hours partial transparent film was developed. The biopolymer electrolyte films were taken from the dishes and then placed in a vacuum desiccator until further tests. The dried bio-polymer films were

characterized by the JASCO V-670 UV-VIS-NIR Spectrophotometer. The effect of the salt in the solid biopolymer electrolyte was observed from the UV-visible studies. It was studied the optical characterizations at room temperature by utilizing a UV-Visible spectrometer.

## Results and Discussion

**Absorption and absorption coefficient studies:** UV spectrum was obtained from the spectrometer under room temperature. UV Spectrometer was used to calculate the absorption spectra of the given sample in the wavelength range of 200-900 nm<sup>17</sup>. The optical absorption study was utilized to investigate the optically induced transition and structure of the sample. The spectrum of optical absorption takes place in the range of 250-330 nm. The absorption spectra of pure and doped NaNO<sub>3</sub> of Polymer electrolytes were shown in fig.2. In biopolymers, several electronic transitions may be occurred<sup>18</sup>. The optical absorption spectra can show sharp increase absorption at a wavelength near to absorption edge for onset optical absorption. The absorption energy is corresponding to this establishes the optical energy bandgap of the material. Structural and optical band gaps are determining with optical absorption studies. Generally, for pure biopolymers no absorption is there but by increasing doping content the absorption is to be increasing gradually.

In each figure for pure TSP polymer the optical absorption is very less, by increasing the salt NaNO<sub>3</sub> concentration absorption is increased gradually and for TSP 70%: NaNO<sub>3</sub> 30% concentration high absorption arrived at the wavelength 290 nm then after again optical absorption is rise down<sup>19</sup>. In the proposed electrolyte at this concentration, the change in the band structure and absorption coefficient is high. The absorption can be calculated by its absorption coefficient ( $\alpha$ ), this is called a fraction of power of absorption of unit length of the material. The absorption coefficient can be calculated by using the given formula<sup>17</sup>.

$$\alpha = (2.3032/d) \times A$$

where A is optical absorption data obtained from the spectrometer, d is the thickness of the pure and doped concentration film<sup>18</sup>.

Fig. 3 represents the optical absorption coefficient versus the energy of photon for pure TSP and NaNO<sub>3</sub> doped concentrations. It is cleared that the absorption edge is high for pure TSP film and it will be decreasing by increasing doping concentration of salt. Finally, for TSP70%: NaNO<sub>3</sub> 30% concentration the absorption edge is minimum and it is shifted towards higher energy above this concentration. The photon energy range is lying from 4.9eV to 4.6eV represents a decrease of the bandgap of the doped samples<sup>20</sup>.

**Transmittance:** Transmission spectra of pure polymer TSP with different concentrations of NaNO<sub>3</sub> were measured in

the wavelength range (200–800 nm) and are shown in fig.4. It is seen that pure TSP has a high optical transmission which decreases by increasing the doped concentration NaNO<sub>3</sub><sup>20</sup>. This effect is due to the structural change in TSP as a result of inter and intra-molecular interactions between TSP polymer chain segments and dopant content NaNO<sub>3</sub>.

The interactions of cations (Na<sup>+</sup>) and anions (NO<sub>3</sub><sup>-</sup>) of salt with electropositive & negative constituents of polar molecules of the TSP matrix takes place<sup>21</sup>. A small transmission band is noticed at about 259 nm. For pure sample the transmittance is very high, by increasing the salt concentration transmittance is decreases gradually and for 70% TSP: 30% NaNO<sub>3</sub> value is very low, from that again its value is rising. This band seems to disappear by irradiation which can be attributed to the interaction between 'Na' ions and the biopolymer chains.

The ratio of radiant power transmitted ( $P$ ) by a sample to the radiant power incident ( $P_0$ ) on the sample is called the transmittance  $T$ .

$$\text{But, } P = P_0 T \\ T = e^{-\alpha t}$$

Where ' $\alpha$ ' is the optical absorption coefficient and ' $t$ ' is the thickness of the sample. Transmission can be calculated from the measured optical absorbance. The transmission spectrum samples from 200-350 nm are shown in fig.4. The reflectance of the film was calculated from optical absorption data 'A' and optical transmission 'T' using the given relation

$$R = 1 - (T + A)$$

**Refractive Index:** The properties of the optical refractive index and optical excitation coefficient can produce an optical constant of the material<sup>22</sup>. Exact optoelectronics applications are related to the produced optical properties such as atomic structure, electronic bond structure and electrical properties.

Fig. 5 shows the refractive index for pure TSP and different NaNO<sub>3</sub> doped concentrations of TSP. The refractive index was calculated from reflectance R and its excitation coefficient K<sup>23</sup>. The relation between refractive index and reflectance is given here at a normal incident of light through the sample. The refractive index is the basic optical property of the material which indicates dispersion at all wavelengths. The most probable refractive index can connect to the electronic polarization. The optical refractive index of a material indicates the molecular and electronic polarization of the electromagnetic field of light.

In the graph, the refractive index is very low and constant for all given samples at lower energy up to 3.5eV, the refractive index was increased by increasing photon energy. From 5eV incident photon energy the refractive index value rapidly

increases for all films. From 5.3 eV again films follow the constant and high refractive index. In these electrolyte films, by increasing the doping concentration the optical refractive index is increased up to 70% TSP: 30% NaNO<sub>3</sub> and showing high value. The reason is due to electronic and molecular polarization will be more, dispersion is also very high value and optical wavelength is lower value.

The equation for reflectance relation is:

$$R = [(n-1)^2 + K^2] / [(n+1)^2 + K^2]$$

Above equation can be written as:

$$n = (1 + \sqrt{R}) / (1 - \sqrt{R})$$

where 'R' is reflectance, 'K' is an extinction coefficient and 'n' is a refractive index of the sample material.

Fig. 6 shows the plots between conductance and photon energy. The conductivity of the sample is depending upon the refractive index and its dispersion nature of the sample. If the moment and rotation of the particles are more consequently material dispersion will be increased, which tends to increase the conductivity of the material. In this work, the conductivity of pure TSP is very less, by increasing the dopant concentration to pure TSP then the conductivity is increased gradually and finally 70% TSP: 30% NaNO<sub>3</sub> has shown the highest value<sup>24</sup>. Optical conductance can be obtained from the refractive index, absorption coefficient and velocity of the light passing through the pure and several doped concentration samples of the material. Optical conductance is to be found by using the relation.

$$\sigma = \alpha n c / 4\pi$$

where 'α' is the absorption coefficient, 'n' is a refractive index of the sample, 'c' is the velocity of the light.

**Extinction Coefficient:** The extinction coefficient (K) is an imaginary part of the optical refractive index was calculated for all pure and doped samples. In given fig. 7 extinction coefficient spectra versus wavelength behaviour is represented, it is seen that the extinction coefficient for pure TSP and several NaNO<sub>3</sub> doped concentrations of TSP<sup>25</sup>. The deviation of extinction coefficient value with wavelength shows such interaction between medium and photon energy. When the incident light is scattering through the specific medium then the fraction of electromagnetic energy loss occurs is known as the extinction coefficient.

As shown in the figure, the extinction coefficient was increased by increasing wavelength and by increasing dopant concentration. The extinction coefficient value is increasing up to 70% TSP: 30% NaNO<sub>3</sub> represents high value, again by increasing salt dopant concentration it will

start to decrease. We can determine the extinction coefficient by the formula.

$$K = \alpha \lambda / 4\pi$$

where 'λ' represents the wavelength of the incident light, 'α' is an absorption coefficient. From this extinction coefficient, the real and imaginary complex parts of dielectric constant values can be determined.

**Energy Band Gap:** The data regarding the band structure of solids is calculated from the optical absorption study. Mainly, the direct band and indirect bandgap are dividing insulators and semiconductor materials into two major parts. In direct band, the conduction and valence band are both situated at the same zero crystal momentum<sup>26</sup>. In an indirect band, the conduction band does not agree to zero crystal momentum. In an indirect bandgap from the valence band to conduction band should always be linked with a phonon of the crystal momentum<sup>27</sup>.

Davis and Shalliday describe that both indirect and direct energy bandgap has occurred near the fundamental band edge and this can be explained by plotting  $(\alpha h\nu)^{1/2}$  and  $(\alpha h\nu)^2$  as a function of photon energy. The transmission, absorption, absorption edge and electron transition from valence band to the conduction band, can be determined by  $(h\nu)$  photon energy<sup>28</sup>.

The absorption bandgap can determine from the graph of  $(\alpha h\nu)$  versus the photon energy  $(h\nu)$  which is shown in fig.8. The energy band gap also can be determined from  $(\alpha h\nu)^x$  versus  $(h\nu)$ . It is determined from a linear portion of the curve to cut 'hν' at the x-axis as shown in figs. 9,10,11. The value of energy band gaps is shown in table 1. The bandgap values obtained from fig.9 and fig.10 are plots for allowed indirect transition ( $x = 2/3$ ) and forbidden indirect transition ( $x = 1/2$ ). From fig.11, the direct energy bandgap ( $x = 2$ ) is obtained. The results indicate that the electronic transition is direct in the present doped samples, is called as optical bandgap.

In this present research work, a bandgap of 5.01eV is obtained for pure TSP. UV-visible data gave information on the optical energy bandgap. Between  $(\alpha h\nu)^2$  versus  $h\nu$  gives the value of the direct bandgap<sup>29</sup>. From the UV-visible spectra, optical absorption decreases by an increase in wavelength.

The absorption edge is obtained from the plot of  $h\nu$  versus  $\alpha$ . Absorption edge, absorption bandgap, direct bandgap, indirect allowed and forbidden gaps are decreased by increasing the doping concentrations are shown in table.1. 70% TSP: 30% NaNO<sub>3</sub> concentration film exhibited a minimum value for all band gaps, from this ratio above mentioned band gaps are increased by increasing the salt concentrations<sup>29</sup>. The energy band gaps are increased in the same above parameters.

Table 1

Absorption edge, Optical refractive index, Forbidden and allowed indirect energy bandgap, direct energy bandgap for pure TSP and TSP: NaNO<sub>3</sub> doped Films

S.N.	Composition	Absorption edge	Absorption bandgap	Forbidden indirect bandgap	Allowed indirect bandgap	Direct bandgap	Refractive index
1	100% TSP: 0% NaNO <sub>3</sub>	4.98	4.91	4.87	4.83	5.01	0.82
2	90% TSP: 10% NaNO <sub>3</sub>	4.85	4.84	4.71	4.71	4.95	0.87
3	80% TSP: 20% NaNO <sub>3</sub>	4.79	4.75	4.56	4.64	4.84	1.41
4	70% TSP: 30% NaNO <sub>3</sub>	4.65	4.64	4.33	4.47	4.65	2.02
5	60% TSP: 40% NaNO <sub>3</sub>	4.72	4.7	4.47	5.59	4.74	1.49

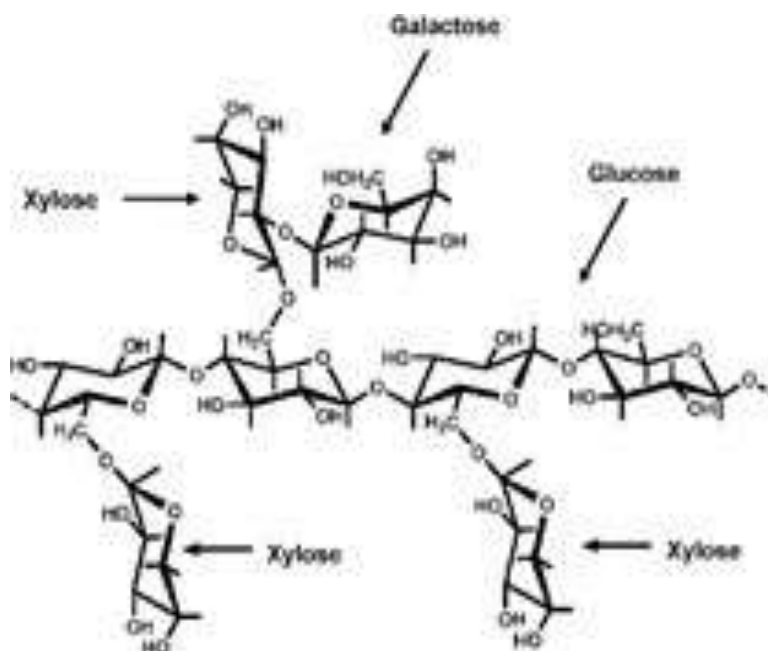


Fig. 1: Molecular structure for Tamarind Seed Polysaccharide (TSP)

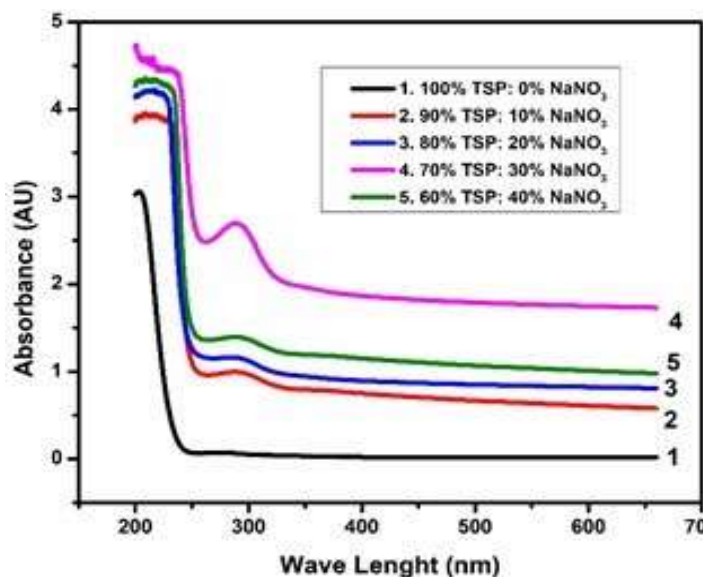


Fig. 2: Optical absorption as a function of wavelength for pure TSP and TSP: NaNO<sub>3</sub> doped electrolytes.

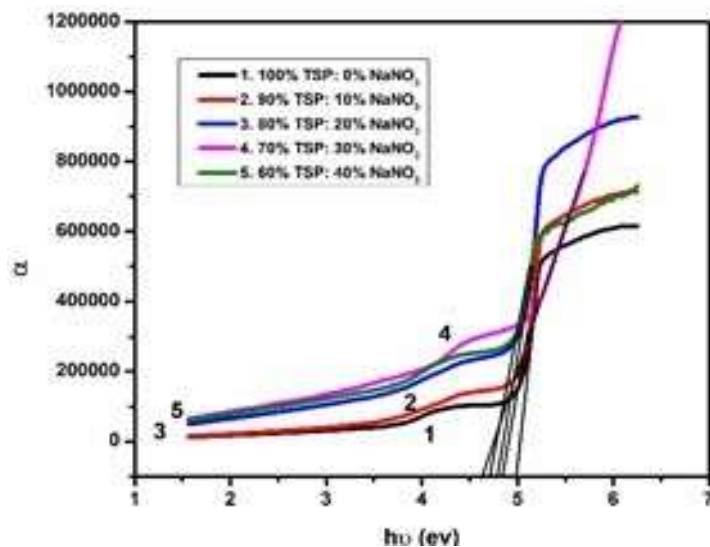


Fig. 3: Optical absorption coefficient as a function of photon energy for pure TSP and TSP: NaNO<sub>3</sub> doped films

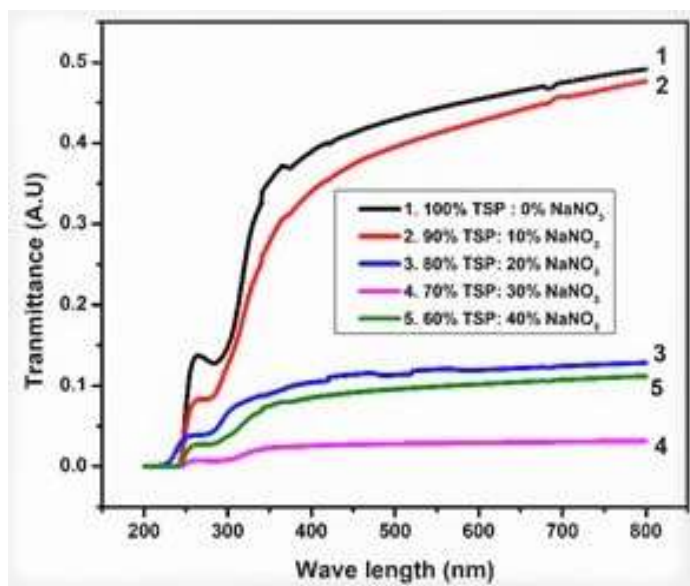


Fig. 4: Optical transmission as a function of wavelength for pure TSP and TSP: NaNO<sub>3</sub> doped films

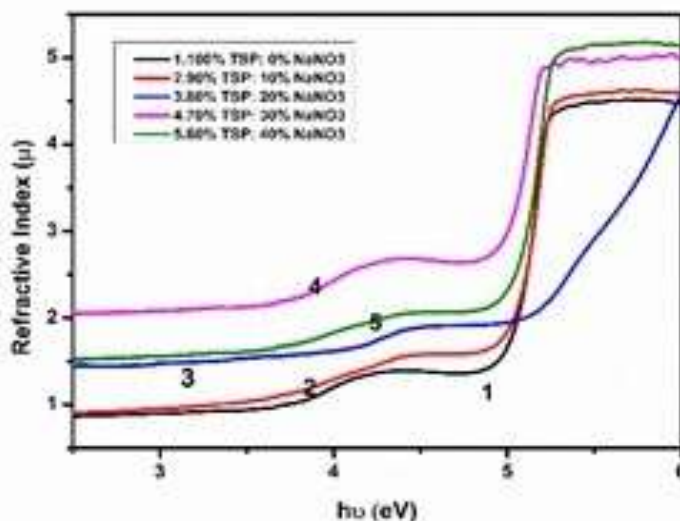


Fig. 5: Optical refractive index as a function of photon energy for pure TSP and TSP: NaNO<sub>3</sub> doped films

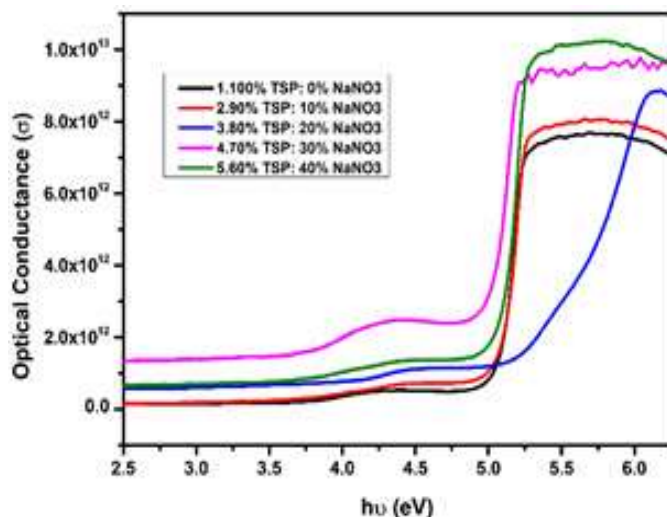


Fig. 6: Optical conductance as a function of photon energy for pure TSP and TSP:  $\text{NaNO}_3$  doped films

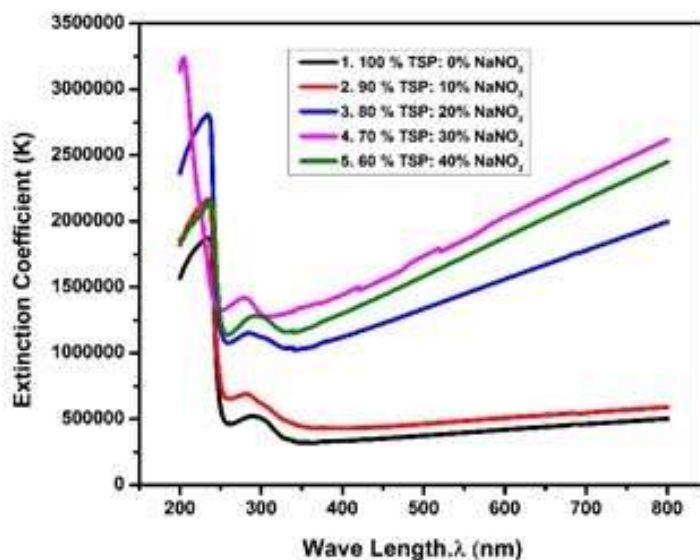


Fig. 7: Extinction coefficient as a function of wavelength for pure TSP and TSP:  $\text{NaNO}_3$  doped films

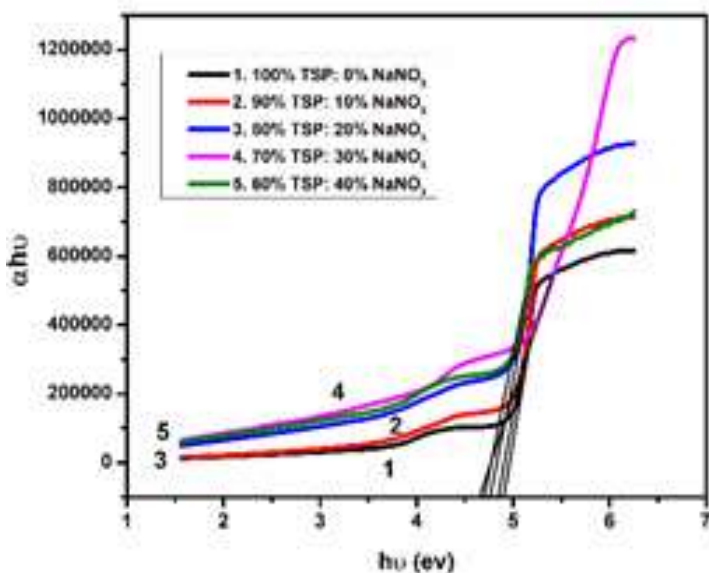


Fig. 8: Plots of  $(\alpha h\nu)$  versus  $(h\nu)$  for pure TSP and TSP:  $\text{NaNO}_3$  doped Films

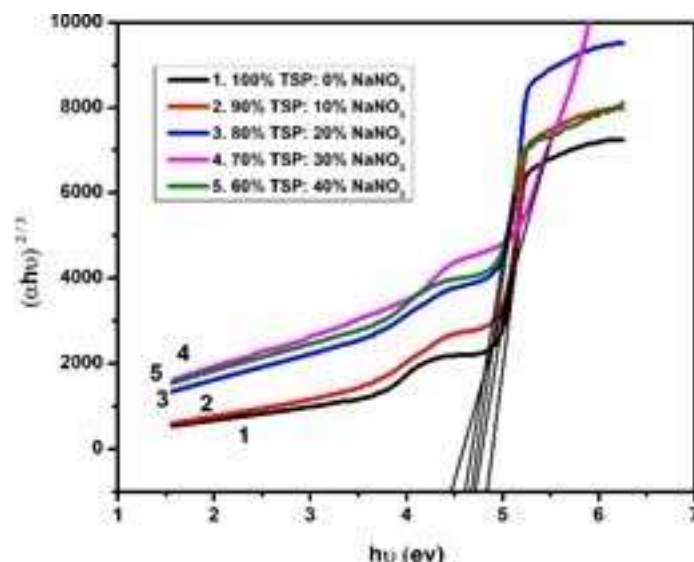


Fig. 9: Plots of  $(\alpha h\nu)^{1/2}$  versus  $(h\nu)$  for pure TSP and TSP:  $\text{NaNO}_3$  doped Films

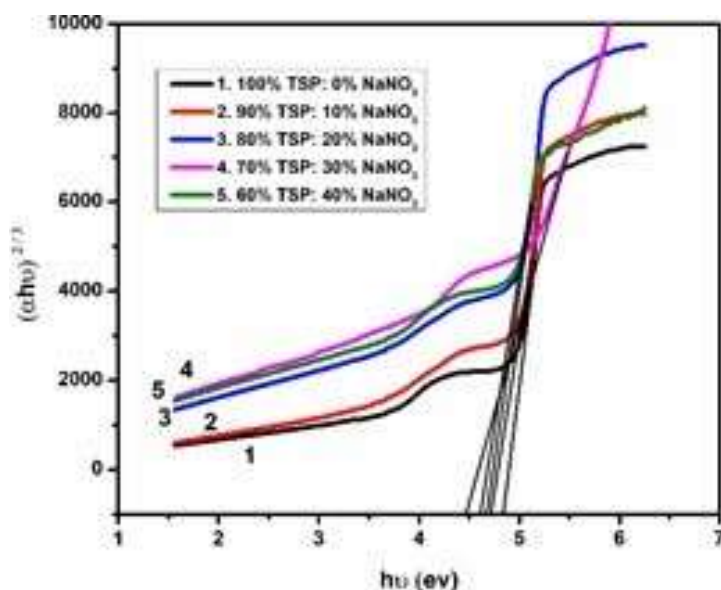


Fig. 10: Plots of  $(\alpha h\nu)^{2/3}$  versus  $(h\nu)$  for pure TSP and TSP:  $\text{NaNO}_3$  doped Films

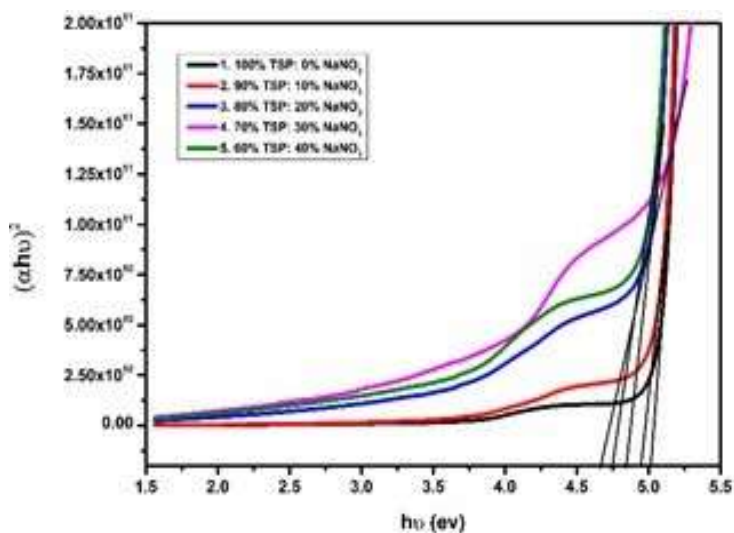


Fig. 11: Plots of  $(\alpha h\nu)^2$  versus  $(h\nu)$  for pure TSP and TSP:  $\text{NaNO}_3$  doped Films

## Conclusion

In this research work, the solid biopolymer electrolyte (SPE) films are prepared with different concentrations of TSP: NaNO<sub>3</sub> (100:0, 90:10, 80:20, 70:30, 60:40 wt.%) using solution casting technique. The study and analysis of optical parameters for doped NaNO<sub>3</sub> based on TSP have been observed and the properties of the film are explained. It is observed that the optical refractive index is increased by increasing the doping content of NaNO<sub>3</sub> into the pure biopolymer TSP. The optical refractive index is changing the conductance of the material and the density of TSP electrolyte is increased with the increase of dopant concentration NaNO<sub>3</sub>. It is observed that the optical conductivity is decreased by decreasing photon energy and it gets finally constant. This suggested that the decrease in the optical conductivity is related to reduce of photon energy. The decreasing energy bandgap ( $E_g$ ) by doping TSP with different wt% NaNO<sub>3</sub> is observed.

Finally, it is observed that by increasing the salt NaNO<sub>3</sub> content to biopolymer TSP then the optical conductance, absorption edge, indirect and direct band gaps are decreased and the refractive index is increased up to 70% TSP: 30% NaNO<sub>3</sub> films.

## Acknowledgement

We would like to thank the department of science and Technology (DST, Delhi), Govt of India for the award of DST-FIST Level-1(SR/FST/PS-1/2018/35) Scheme to the Department of Physics, KLEF. Thanks and grateful to the KLEF providing infrastructure facilities (Perform basic instruments) and support to conduct research.

## References

1. Krishna Jyothi N., Venkataratnam K.K., Narayana Murty P. and Vijayakumar K., Preparation and Characterization of PAN-KI Complexed gel Polymer Electrolytes for solid state battery application, *Bullen of Materials Science*, **39(4)**, 1047-1055 (2017)
2. Bouchet R., Maria S., Meziane R., Aboulaich A., Lienafa L., Bonnet J.P., Trang N.T.P., Bertin D., Gigmes D. and Devaux D., Single-ion BAB triblock copolymers as highly efficient electrolytes for lithium-metal batteries, *Nat Mater*, **12(1)**, 452–457 (2013)
3. Rajeswari N., Selvasekarapandian Karthikeyan S.S., Nithya H. and Sanjeeviraja C., Lithium ion conducting polymer electrolyte based on poly (vinyl alcohol)–poly (vinyl pyrrolidone) blend with LiClO<sub>4</sub>, *Int J Polym Mater Polym Biomaterial*, **61(14)**, 1164–1175 (2012)
4. Quartarone E. and Mustarelli P., Electrolytes for solid-state lithium rechargeable batteries: recent advances and perspectives, *Chem. Soc. Rev.*, **40**, 2525–2540 (2011)
5. Huang B., Wang Z., Li G., Huang H., Xue R., Chen L. and Wang F., Lithium ion conduction in polymer electrolytes based on PAN, *Solid State Ionics*, **85**, 79–84 (1996)
6. Smith D.M., Dong B., Marron R.W., Birnkrant M.J., Elabd

Y.A., Natarajan L.V., Tondiglia V.P., Bunning T.J. and Li C.Y., Tuning ion conducting pathways using holographic polymerization, *Nano. Lett.*, **12**, 310–314 (2011)

7. Dragunski D.C. and Pawlicka A., Starch based solid polymeric electrolytes, *Mol Cryst Liq Cryst*, **374**, 561–568 (2002)

8. Majid S.R. and Arof A.K., Proton-conducting polymer electrolyte films based on chitosan acetate complexed with NH<sub>4</sub>NO<sub>3</sub> salt, *Phys B Condens Matter*, **355**, 78–82 (2005)

9. Ahmad Khair A.S. and Arof A.K., Electrical properties of starch/ chitosan-NH<sub>4</sub>NO<sub>3</sub> polymer electrolyte, *Ionics*, **16**, 123–129 (2010)

10. Hodge R.M., Edward G.H. and Simon G.P., Water absorption and states of water in semicrystalline poly (vinyl alcohol) films, *Polymer*, **37**, 1371–1376 (1996)

11. Smith D.M., Dong B., Marron R.W., Birnkrant M.J., Elabd Y.A., Natarajan L.V., Tondiglia V.P., Bunning T.J. and Li C.Y., Tuning ion conducting pathways using holographic polymerization, *Nano Lett*, **12**, 310–314 (2011)

12. Andrade J.R., Raphael E. and Pawlicka A., Plasticized pectinbased gel electrolytes, *Electrochim Acta*, **54**, 6479–6483 (2009)

13. Raphael E., Avellaneda C.O., Manzolli B. and Pawlicka A., Agar based films for application as polymer electrolytes, *Electrochim Acta*, **55**, 1455–1459 (2010)

14. Osman Z., Ibrahim Z.A. and Arof A.K., Conductivity enhancement due to ion dissociation in plasticized chitosan-based polymer electrolytes, *Carbohydr Polym*, **44**, 167–173 (2001)

15. Smith D.M., Dong B., Marron R.W., Birnkrant M.J., Elabd Y.A., Natarajan L.V., Tondiglia V.P., Bunning T.J. and Li C.Y., Tuning ion conducting pathways using holographic polymerization, *Nano Lett*, **12**, 310–314 (2011)

16. Hashmi S.A., Kumar A., Maurya K.K. and Chandra S., Proton conducting polymer electrolyte, I, The polyethylene oxide + NH<sub>4</sub>ClO<sub>4</sub> system, *J. Phys. D. Appl. Phys.*, **23**, 1307 (1993)

17. Rajendran S., Ramesh Prabhu M. and Usha Rani M., Ionic Conduction in Poly(vinyl chloride)/poly(ethyl methacrylate)-based polymer blend electrolytes complexed with different lithium salts, *J. Power Sources*, **180**, 880-883 (2008)

18. Morsi M.A. and Abdelghany A.M., UV-irradiation assisted control of the structural, optical and thermal properties of PEO/PVP blended gold nano particles, *Mater. Chem. Phys.*, **201**, 100-112 (2017)

19. Muthuvinnayagam M. and Gopinathn C., Characterization of proton conducting polymer blend electrolytes based on PVDF-PVA, *Polymer*, **68**, 122-130 (2015)

20. Das R. and Pandey S., Comparison of optical properties of bulk and nano crystalline thin films of CdS using different precursors, *Int. J. of Mater. Sci.*, **1(1)**, 35-40 (2011)

21. Raja V., Sarma A.K. and Narasimha Rao V.V.R., Optical

properties of pure and doped PMMA-CO-P4VPNO polymer films, *Mater. Lett.*, **57(30)**, 4678-4683 (2003)

22. Ballato J. and Foulger S., Optical Properties of Perfluorocyclobutyl Polymers, *J. of Opt. Soc. of Am.*, **B20(9)**, 1838-1843 (2003)

23. Abdullah O.Gh. and Saber D.R., Optical absorption of polyvinyle alcohol films doped with Nickel Chloride, *Appl. Mech. and Mater.*, **110-116**, 177-182 (2012)

24. Chandrakala H.N., Ramaraj B., Shivakumaraiah and Madhu G.M., Siddaramaiah, *J. Mater Sci*, **47**, 8076-84 (2012)

25. Indulal C.R., Vaidyan A.V., Kumar G.S. and Raveendran R., Characterization, dielectric and optical studies of nano-ceramic phosphor iodate synthesized by chemical co-precipitation method, *Indian J. of Eng. & Mater. Sci.*, **17**, 299-304 (2010)

26. Abdullah O.G.H. and Muhammad D.S., Physical properties of pure and copper oxide doped polystyrene films, *Int. J. of Mater. Sci.*, **5(4)**, 537-545 (2010)

27. Bhajantri R.F., Ravindrachary V., Harisha A., Ranganathaiah C. and Kumaraswamy G.N., Effect of barium chloride doping on PVA microstructure: positron annihilation study, *Appl Phys A*, **87**, 797-805 (2007)

28. Shehap A.M., Thermal and Spectroscopic Studies of Polyvinyl Alcohol/Sodium Carboxy Methyl Cellulose Blends, *Egypt. J. Solids*, **31(1)**, 75-91 (2008)

29. Modreanu M., Gartner M. and Tomozeiu N., Optical characterization of LPCVD SiOxNy thin films, *Proc. Electrochem. Soc.*, **1**, 118-129 (2003).